J Mater Sci: Mater Med (2006) 17:717–726
DOI 10.1007/s10856-006-9682-z

Electron microscopic investigation on the osteogenesis at titanium implant/bone marrow interface under masticatory loading

H. Kawahara · S. Nakakita · M. Ito · K. Niwa · D. Kawahara · S. Matsuda

Received: 27 July 2004 / Accepted: 24 October 2005

Abstract Electron microscopic investigation on osteogenetic process at the implant surface of threadless rod-type titanium implants with different surface roughness of Ra 0.4 $\pm$ 0.01 μm, Sm 2.6 $\pm$ 0.3 μm and Ra 2.0 $\pm$ 0.12 μm, Sm 36 $\pm$ 9.1 μm was performed at the early stage of 21 and 42 days post implantation into the jawbones of four beagles under the load bearing condition of functional mastication. The implant surfaces were covered with a blood clot and haematopoietic stem cells (HSC) including phagocytic monocytes immediately after the implantation. Successively, osteogenic stem cells (OSC) migrated from cortical and/or trabecular endosteum to the HSC-layer on the implant surface. The new bone formation at the implant/bone marrow interface was developed by collaboration of osteomediator cells (OMC) differentiated from monocytes of HSC and osteoblast phenotype cells of OSC derived from endosteum of cortical bone and/or trabecular. The new bone layer at the implant surface consisted of two layers, solution-mediated calcification layer of pseudo bone and cell (osteoblast) -mediated calcification layer of true bone. The pseudo bone was produced by solution-mediated calcification of OMC- and HSC-remnants near by the implant surface. The bone healing process at the implant/bone marrow interface depended upon two factors; the migration of OSC from cortical and/or trabecular endosteum to the implant surface and the healing potentiality. Topographic dependency upon the bone healing potential at implant/bone marrow interface was not confirmed in this experiment under the load bearing condition of functional mastication.

H. Kawahara (✉) · S. Nakakita · K. Niwa · D. Kawahara
Institute of Clinical Materials, 1-22-27 Tokocho, Moriguchi, Osaka 570-0035, Japan
e-mail: icm@sea.plala.or.jp

M. Ito · S. Matsuda
Ehime University School of Medicine, Sitsukawa, Shigenobu, Ehime 791-0295, Japan

Introduction

In vivo studies on osteogenesis at the implant/bone interface have been reported by many references while number of studies have been performed under non-clinical condition without masticatory loading. For the purpose of predicting quality of dental implants, the animal experiment should be performed under the clinical condition of masticatory loading with superstructure of metallic crown and bridge. Kawahara et al. reported that osseointegration developed at implant/bone interface under the functional loading of mastication, when the implant was rigidly fixed with micromotion less than 50 μm [1, 2]. This study was carried out by light and electron microscopic investigations using beagles to clarify topographic dependency on osteogenetic process at the titanium implant/bone marrow interface under the load bearing condition of functional mastication.

Materials and methods

Implants: Rod type implants of 2mm diameter and 12mm length were made of cp titanium (Japanese Industrial Standards, H4600, grade 2 ⟨H, 0.013 under; O, 0.2 under; N, 0.05 under; Fe, 0.25 under⟩, Toho Titanium Co., Ltd., Chigasaki, Japan). Two different surface roughness of small roughness, SR (Ra 0.4 $\pm$ 0.01 μm, Rz 2.9 μ0.16 μm, Rmax 3.6 $\pm$ 0.36 μm, Sm 2.9 $\pm$ 0.3 μm) and large roughness, LR (Ra 2.0 $\pm$

0.12 μm, Rz 11.2 $\pm$ 0.58 μm, Rmax 29.1 $\pm$ 8.6 μm, Sm 39.2 $\pm$ 9.1 μm) were made by 60 sec. etching endosseous part of the implants with 4% hydrofluoric acid solution and 15 sec. pickling with 8% hydroperoxide solution containing 4% hydrofluoric acid for the SR implants, and 120 sec. etching with 4% hydrofluoric acid solution and 15 sec. pickling with 8% hydroperoxide solution containing 4% hydrofluoric acid after corundum blasting for the LR implants [2–3]. Topography of the implant surface treated by corundum blasting, and/or hydrofluoric acid etching demonstrated gathering craters with 2.9 ± 0.3 μm diameter, 2.9 ± 0.1 μm depth in SR and 39.2 $\pm$ 9.1 μm diameter, 11.2 $\pm$ 0.58 μm depth in LR, which were investigated by electron scanning microscopy and mechanical stylus profilometry. The final treatment of 8% hydroperoxide solution containing 4% hydrofluoric acid could improve the implant surface in better compatibility, because of preventing effect upon progress of micro-corrosion at small pits in bottom of craters and rounding effect upon sharp outer rim of craters [4].

Eight implants each of SR and LR were implanted into jawbones, 6 months after extraction of teeth P_3 and P_4 in two beagles, 12 month-old, male, 9.3 & 9.8 kg weight. The health condition and ethic permission were certified by the Ethics Committee on Animal Experimentation, Ehime University School of Medicine. The implants were combined immediately with the proximal teeth P_2 and M_1 with metallic crown bridge made of Au-Pd-Ag alloy to fix the implants [1].

The dogs were sacrificed by perfusing 3% glutaraldehyde solution with 0.2 M cacodylate buffer in pH 7.4 through the carotid artery at 3 and 6 weeks post implantation. After removing the crown bridge sixteen tissue blocks including one of each implant were obtained from the mandibles and refixed with 3% glutaraldehyde solution. The tissue blocks were cut into two pieces at the center of implant longitudinally. The half cut blocks were used for light microscopic observation and the other half for electron microscopic investigation.

Light microscopy: Observation on osteogenesis at the implant/bone marrow interface was performed with non-decalcified specimens including the implant by light microscopy (ECLIPSE, E400, Nikon, Tokyo). The half cut tissue blocks were embedded in epoxy resin (EPON 812, TAAB) after dehydration through a series of graded ethanol and finished by grind section as the microscopic specimen in 30–50 μm thickness with ISOMET Low Speed Saw (BUEHLER, Lake Blutt, USA). These ground specimens were stained with HE and toluidine blue.

Transmission electron microscopy (TEM) : After removing the implant non-decalcified half cut blocks were cut into small pieces near the implant surface. The small pieces were post-fixed with 1% O_sO_4 buffered with 0.1 M cacodylate in pH 7.4 for 2 hours and embedded in the epoxy resin for ultra-thin sectioning of LKB ultra-tome. The ultrathin sections were double stained with 8% uranyl acetate and 10% lead citrate. TEM investigation was performed with Hitachi HU-600 (Hitachi, Tokyo, Japan).

Electron probe microanalysis and X-ray diffractometry: Elemental analysis of calcium and phosphorus with EPMA X-650, Hitachi, Tokyo and micro X-ray diffractometry with RINT-2500, Rigaku, Tokyo were carried out to clarify the calcification aspects at the implant/new bone interface using the half cut tissue block samples.

Results

Light microscopy

Endosteum cells migrated to the implant surface from cortical and/or trabecular envelop including osteogenic stem cells (OSC) and produced cell layer at the implant surface, 3 weeks post implantation. The cell layer of 25–150 μm thickness was constructed by a migration of OSC from the endosteum

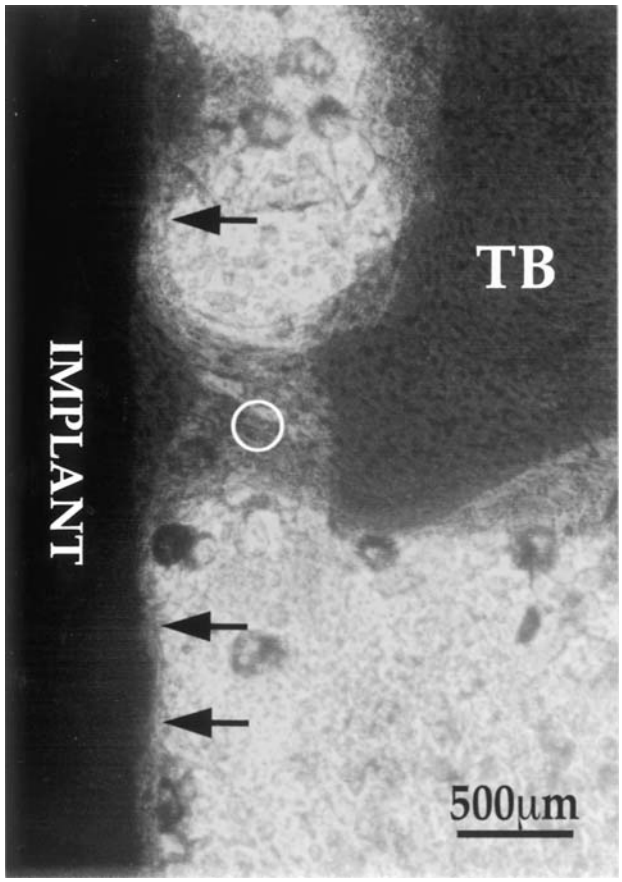

Fig. 1 Implant surface covered by migration of endosteum cells (○) from drill cut edge of adjacent trabecular bone (TB), 3 weeks post implantation of LR (large roughness, Ra 2.0 μm).

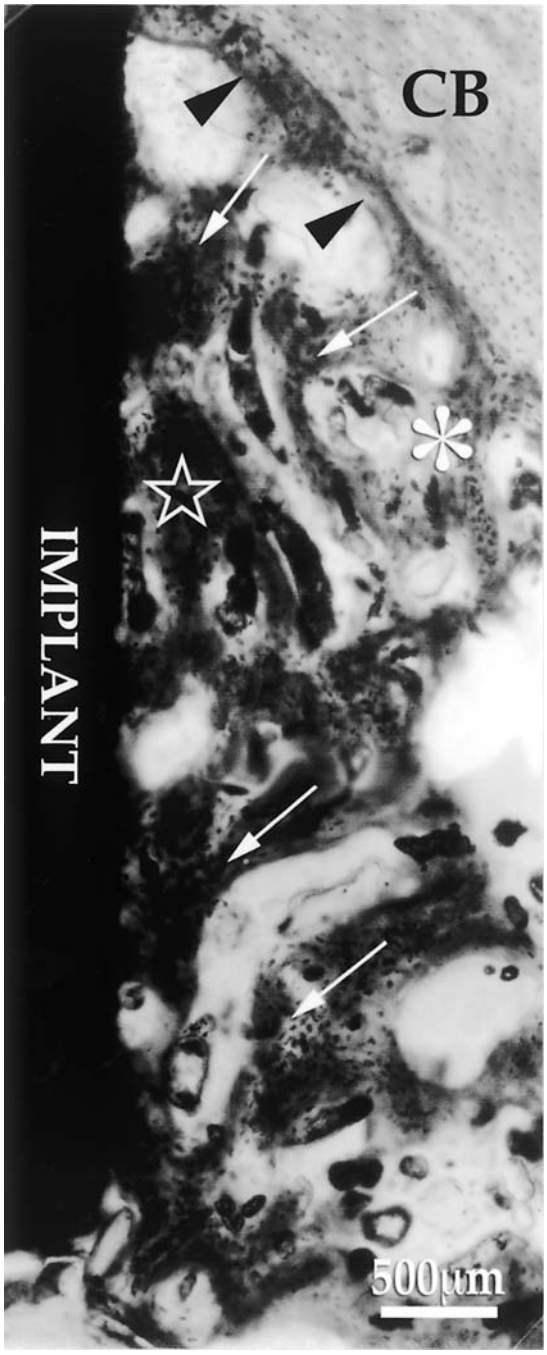

Fig. 2 Active migration of OSC (white arrow) from endosteum (arrow head) of cortical bone (CB) to the implant surface, 3 weeks post implantation of SR (small roughness, Ra 0.4 μm).

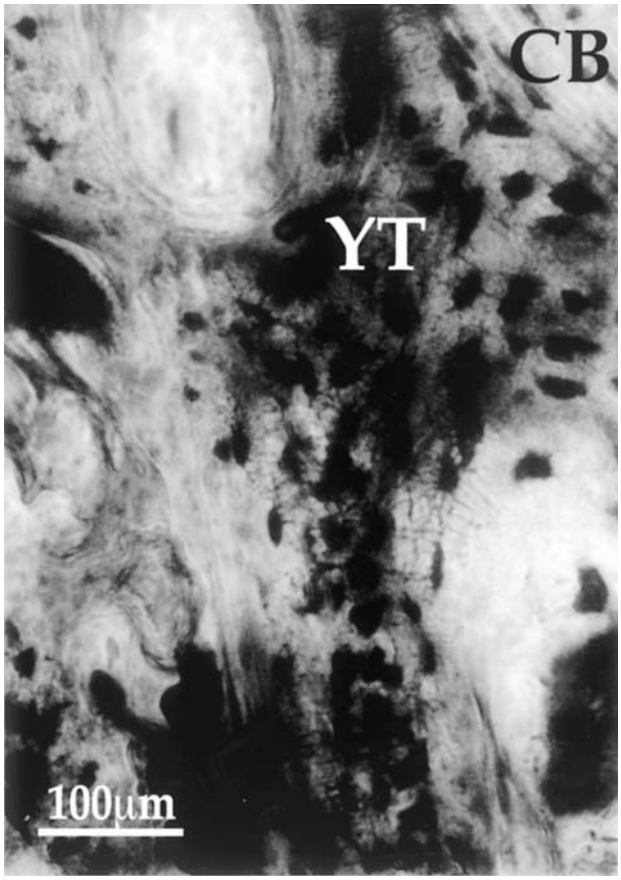

Fig. 3 Large magnification at white aster mark in Figure 2, young trabecular bone (YT) including HSC, OSC, osteoblasts and osteocytes developing into the interspace of fatty marrow.

of adjacent bones (trabecular and/or cortical) to the implant surface covered prior with adhesive contact of haematogenic stem cells (HSC) (Figs., 1–5). New bone formation at the implant surface was performed mainly by migration of OSC from the endosteum of alveolar cortical bone rather than the adjacent trabecular bone especially in the case of poor trabecular bone. The migration from the endosteum of cortical bone to the implant surface was concerned as a main factor to dominate the new bone formation at the implant/bone marrow interface. However, no significant difference were roughly perceived between the both migration of SR and LR.

Transmission electron microscopy

3 weeks post implantation: At the most early stage the implant surface was covered by clotting of HSC including phagocytic monocytes that possessed pluripotential for the cell-differentiation, e.g. to macrophage, osteoclast and osteomediator cell (OMC). OSC migrated from the endosteum of adjacent bones (trabecular and cortical) to the HSC layer prior adhered and covered to the implant surface. Then, OSC could differentiate to osteoblasts through preosteoblasts with cooperation of growth factors released from the OMC (Figs. 6–9). The osteoblasts commenced release of matrix vesicles from their cytoplasmic processes to produce the new bone layer at the implant surface remaining the non-calcified layer 5–40 μm thickness of blood-clot-relic of HSC remnants (Figs. 10, 11). Then calcified layer of

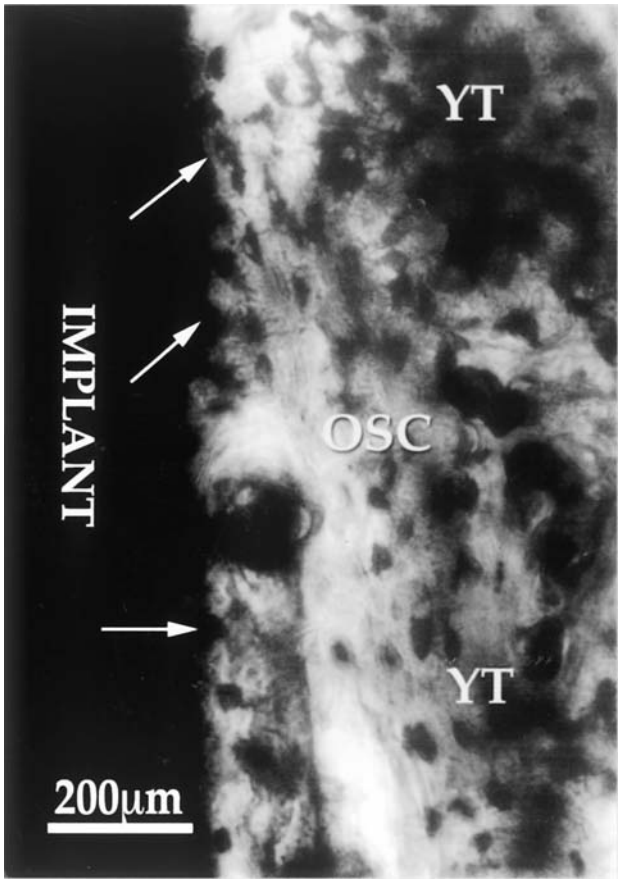

Fig. 4 Large magnification at star mark in Figure 2, OSC migration covers HSC layer (arrows) adhered to the implant surface prior (white arrow), producing new bone layer at the implant surface; OSC, osteoblasts and pre-osteocytes are seen in young trabecular bone (YT).

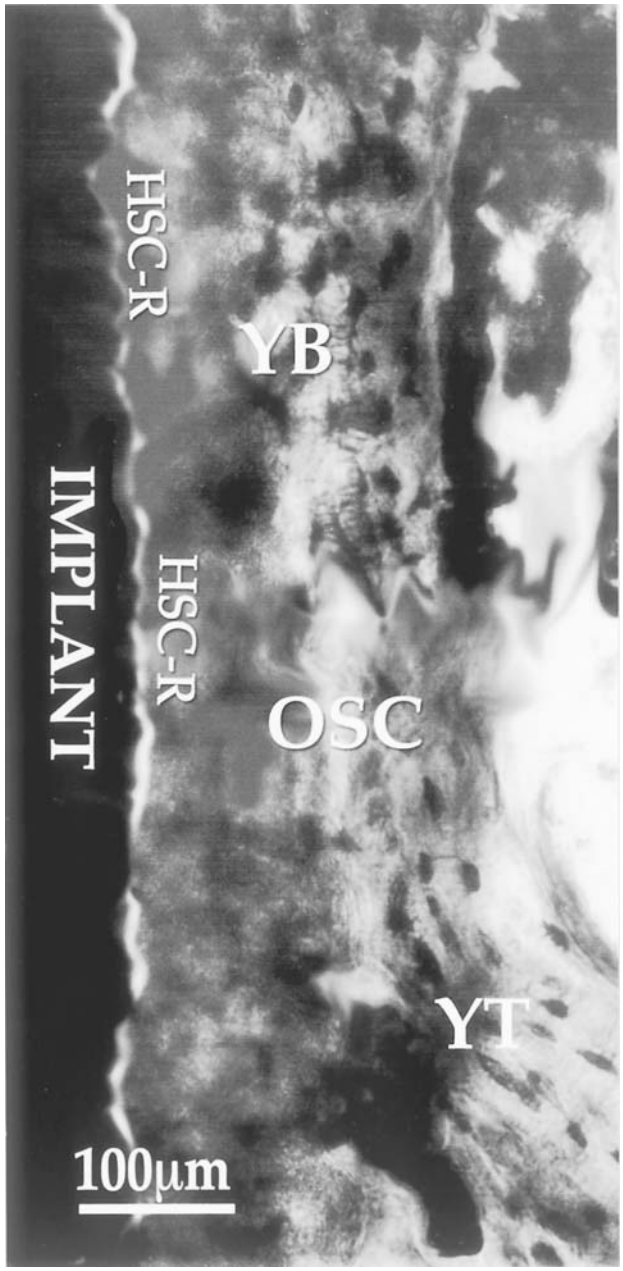

Fig. 5 OSC migration covers HSC or HSC-remnant layer (HSC-R) formed prior at the implant surface and produces young bone (YB) by collaboration of HSC at the implant surface (see Figure 6); Separation between the implant and HSC-R layer is artefact. 3 weeks post implantation of LR.

new bone followed the HSC remnant layer contacted to the implant surface with electron dense membrane, 20–100nm thickness.

6 weeks post implantation: Preosteocytes and osteocytes were invested in collagen fibres layer and its calcified layer of new bone. Osteoblasts oriented in parallel to longitudinal direction of the collagen fibres layer attending their extracellular matrix of 10–20 μm thickness (Fig. 12), when the cytoplasmic processes of osteoblasts extended into the extracellular matrix and collagen fibres layer and developed mineralization of the collagen fibres layer to growth new bone layer (Figs. 6–9 and 13). As time proceeds HSC remnant layer including OMC was calcified by solution-mediated calcification and changed to pseudo bone layer and combined seamlessly to the new bone layer of true bone produced by osteoblast (cell)-mediated calcification. Therefore it is hard to find living OMC in the TEM investigations at 6 weeks post implantation (Fig. 12, 13).

Electron probe microanalysis and X-ray diffraction: In the pseudo bone of solution-mediated calcification layer (SMCL) the electron probe microanalysis demonstrated calcium deposition with low density of phosphorus. The X-ray diffraction spectra indicated an amorphous pattern, unlike the crystalline structure of hydroxyapatite in the true bone of cell (osteoblast) -mediated calcification layer (CMCL), (Figs. 14–16).

The light- and electron-microscopic investigations could clarify morphologically the process and mechanism of

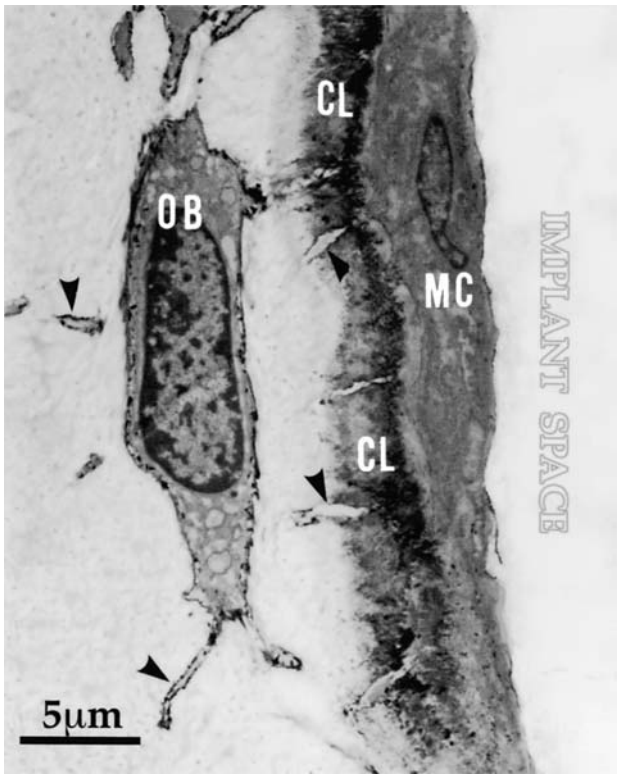

Fig. 6 TEM demonstrates osteomediator cell (MC) between calcified layer (CL) and implant space, MC contacts to the implant surface with 20–100 nm thick electron dense membrane, MC-mediated osteoblast (OB) produces calcified layer (CL) by HA deposition in microfibrils around the MC with matrix vesicles (see Figure 9) released from the cytoplasmic processes of OB (arrow head), 6 weeks post implantation of SR.

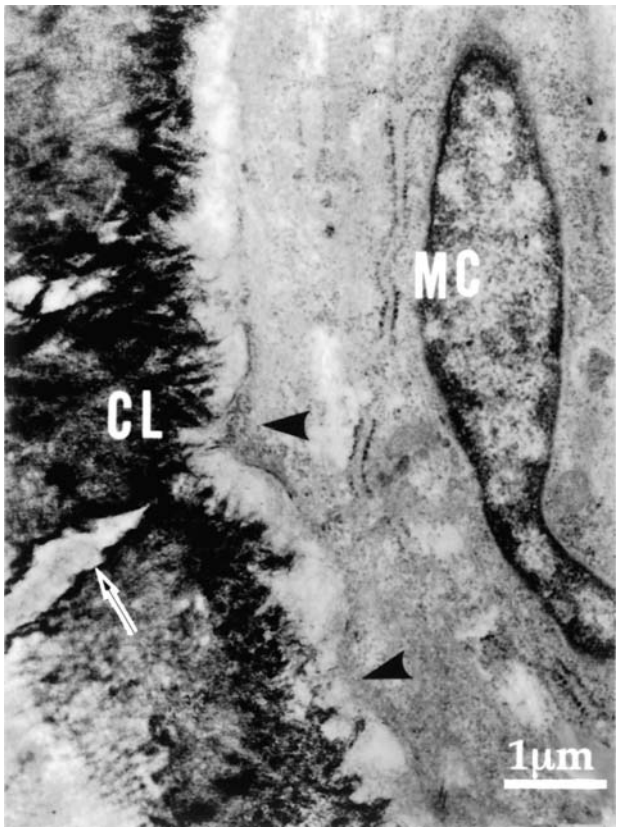

Fig. 7 Large magnification of MC in Figure 6. MC takes slender shape, flattened nucleus and enlarged ER. Cytoplasmic protrusions (arrow head) are releasing electron dense particles to vicinity of osteoblastic process (arrow). Early HA deposition demonstrates beginning of calcified layer (CL).

osteogenesis at the implant/bone marrow interface, while unfortunately the topographic dependency on the bone formation of SR and LR could not be cleared statistically, because small number of samples and wide deviation of the data probably caused by functional mastication under the immediate loading.

Discussions

The surface of dental implants projecting into bone marrow through cortical bone is covered usually with lamellate bone, called "implant sheath bone" [1]. What's the forming process of the implant sheath bone? Firstly, migration of bone formative group cells consisting of haematogenic stem cell (HSC) and osteogenic stem cell (OSC) develops toward the implant surface from the intramedullary tissue including endosteum cells of trabecular and cortical envelop. Secondary, HSC and OSC differentiate to osteomediator cell and osteoblast at the implant/bone marrow interface, and produce the implant sheath bone [2, 3]. Roberts et al. [5] and Gross et al. [6] reported that haematoma-layer was formed on the implant surface at the first stage, and chemical products caused by biochemical reaction at the implant/bone marrow interface, acted on surviving cells and attracted the cells to the implant surface from surrounding tissues including endosteum of cortical and trabecular envelop. Sennerby et al. [7, 8] reported that 7 and 14 days post implantation, new bone appeared as solitary "island" not in contact with the implant, then fused with new trabecular bone originating from the endosteum projecting toward the implant. These processes contributed to the formation of bone collar (the implant sheath bone) surrounding the intramedullary portion of the implant [5–9].

Cell adhesion to the implant surfaces has an influence upon the cell growth, differentiation and tissue morphogenesis [10, 11]. In vitro studies have confirmed close relationship between cell adhesion and cell differentiation [12–15]. Kawahara et al. have demonstrated that cooperative work of osteoblastic phenotype cells originated from OSC and OMC differentiated from phagocytic monocytes of HSC developed the osteogenesis on titanium surfaces, proved by

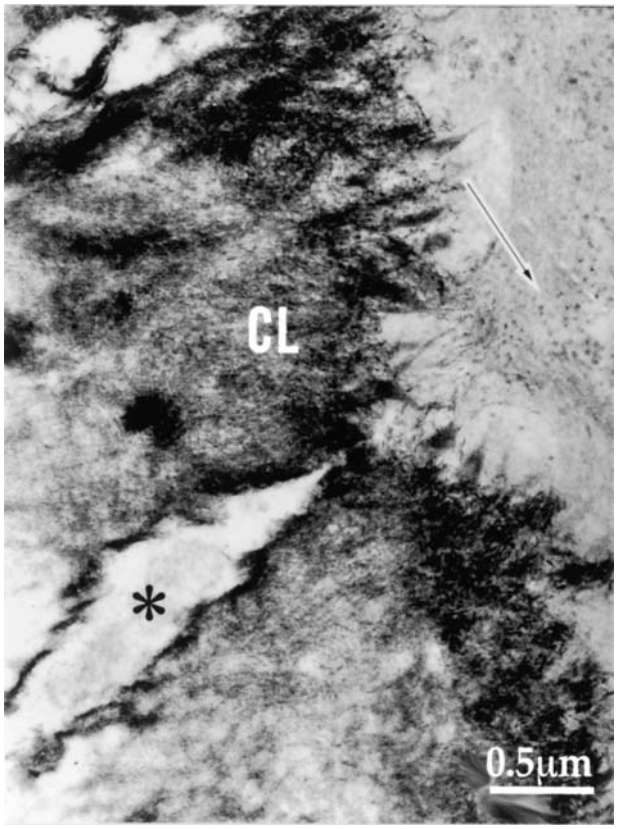

Fig. 8 Large magnification of Figure 7, electron-dense particles (arrow) disperse toward osteoblastic process (✱) through CL, needle-shape HA crystal deposition in microfibrils.

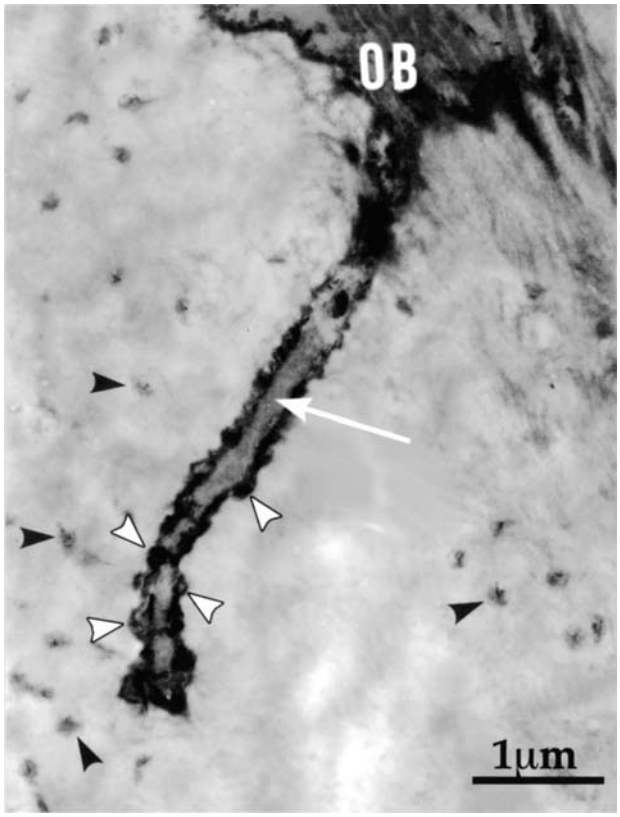

Fig. 9 Large magnification of cytoplasmic process of osteoblast (OB) in bottom part of Figure 6, a number of matrix-vesicles (black arrow heads) and functional germinations of matrix-vesicles (white arrow heads) on the unit-membrane of the process (white arrow).

investigation on architechtural changes of actin filaments, microtubules and cell-organella in the cells closely adhered to the titanium surface. And the cell differentiation from HSC and OSC to osteomediator cell and osteoblasts at the implant surface was assumed from the display of alkaline phosphatase activity and osteocalcin production [3]. These in vitro studies were persuasive on gene expression caused by biomechanical stress to HSC and OSC, that cytoplasmic tension caused by cell adhesion to biomaterials surface may change one of the triggers for the cell differentiation in vivo.

In vivo studies have clarified the effect of surface topography upon cell-adhesion, - proliferation and -differentiation [16–25] and demonstrated that biocompatible implant surfaces were usually covered with the implant sheath bone generated by osteogenesis with the implant/bone marrow interface kinetics [26, 27]. TEM investigations have evidenced flattened cells closely adhered to titanium implant surfaces, e.g. the slender cell of osteoblast like cell reported by Ayukawa et al. [28] and the spindle-shaped mesenchymal cell by Sennerly et al. [7, 8]. Bone forming potential at the implant surface has been discussed from biomechanical standpoint in vitro and in vivo, and the mechanosensitivity of bone controlled with mechanostate of gene-expression on the OSC of periosteum and endosteum has been explained by Frost [29] and Kawahara [1]. In vitro and in vivo studies demonstrated that cell differentiation of intramedullary cells expressed and promoted by nano-structural changes of cytoskeleton and cell-organella caused by mechanical tension with cytoplasmic stretching of cell adhesion to the implant surface [3, 27]. Phagocytic monocytes of HSC differentiated to osteomediator cells (OMC) by the cytoplasmic stretching and OMC mediated and promoted cell differentiation from OSC to osteoblast at the implant surface. Then osteogenesis might to be performed by coupling work of both cells at the implant/bone marrow interface to produce the implant sheath bone.

3 weeks post implantation: A few in vivo studies on the bone healing process at the early stage up to 42 days post implantation have been reported [7, 8]. Dehert et al. [26] investigated the interface kinetics for new bone formation at implant/cortical bone interface in early stage of 7 to 28 days post implantation using rabbit's tibia. Ayukawa et al. [28] reported cellular responses to rod-type titanium implant in early stage of 28 days post implantation. The report identified existence of elongated cells with amorphous proteoglycan membrane of 20–40 nm thickness at the implant/cells interface. These cells have been called

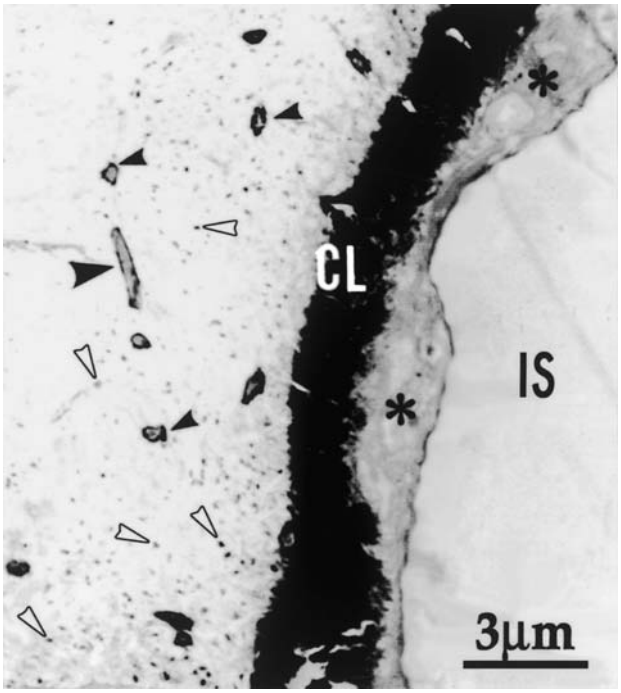

Fig. 10 TEM demonstrates cellular remnants of HSC (✱) including platelets and monocytes between CL and implant space (IS), contacting to the implant surface with 20–100 nm thick electrodense membrane, cytoplasmic processes of osteoblasts (▲) and matrix-vesicles (△) in the extracellular matrix. 3 weeks post implantation of LR.

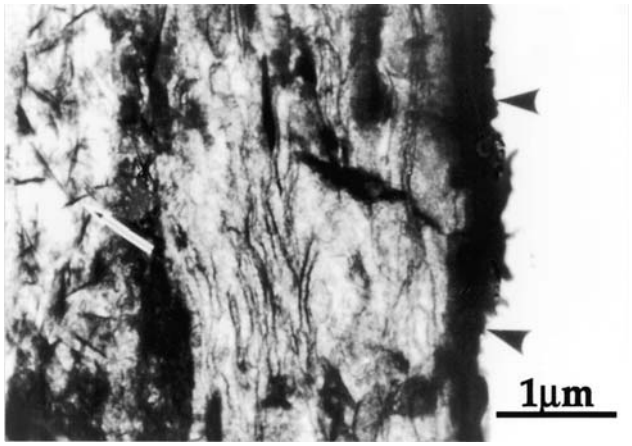

Fig. 11 Degenerated cell-organella in HSC-remnant adhered to the implant surface with electrodense membrane (arrow heads), HA crystals (arrow) in the beginning of osteoblastmediated calcification, 3 weeks post implantation of LR.

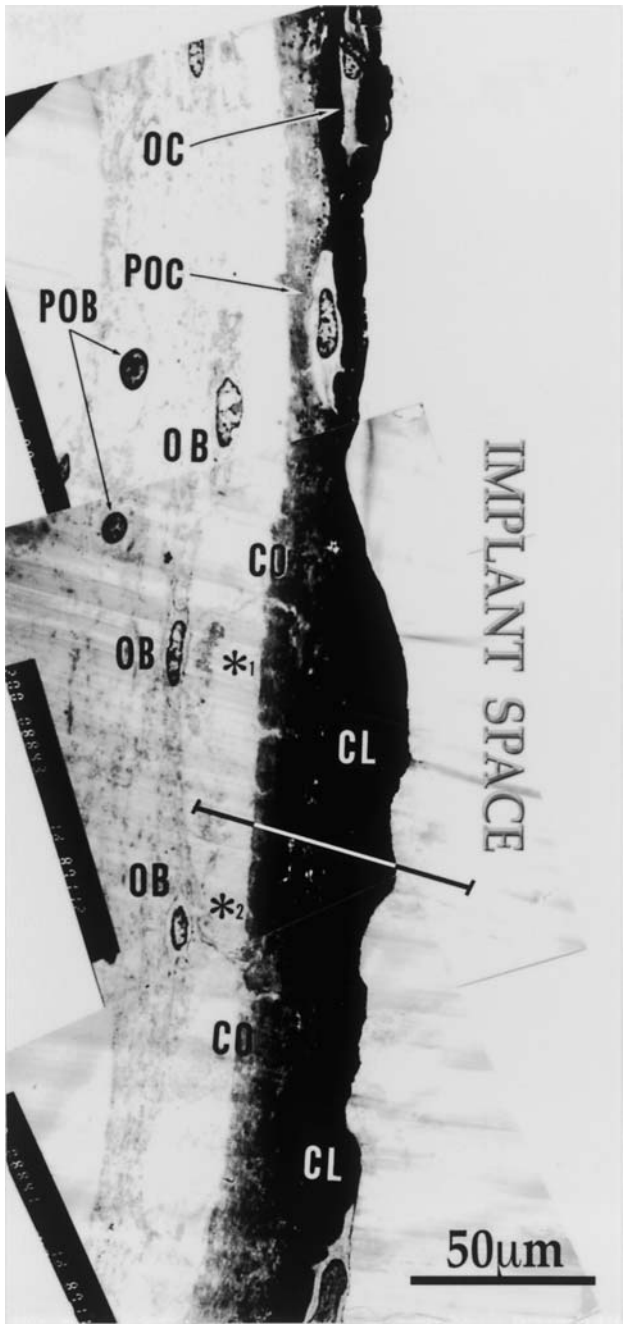

Fig. 12 Calcification progress at the implant surface, osteocyte (OC) and preosteocyte (POC) are invested in calcified layer (CL) and collagen fibres layer (CO), osteoblasts (OB) line up in parallel with the collagen fibres, followed by preosteoblasts (POB) or OSC, 6 weeks post implantation of LR.

osteoblast-like cells, slender cells [28] or elongated mesenchymal cells [7, 8, 30], which probably corresponded to the osteomediator cells (OMC, Figs. 6–8).

OMC was differentiated from phagocytic monocytes of HSC with pluripotentiality for cell differentiation, allowing a balance of bone formation/resorption. TEM demonstrated that OMC could release electron dense particles, which seemed to contain factors of cytokine for OSC differentiation to osteoblast (Figs. 8–11), although such findings were not found out constantly in the electron-microscopic investigations. On the other hand, in vitro study demonstrated that the phagocytic monocyte might differentiate to OMC as metamorphosis on the way of differentiating cascade from phagocytic monocyte to macrophage or osteoclast [3]. It is revealed that the new bone formation at the implant surface

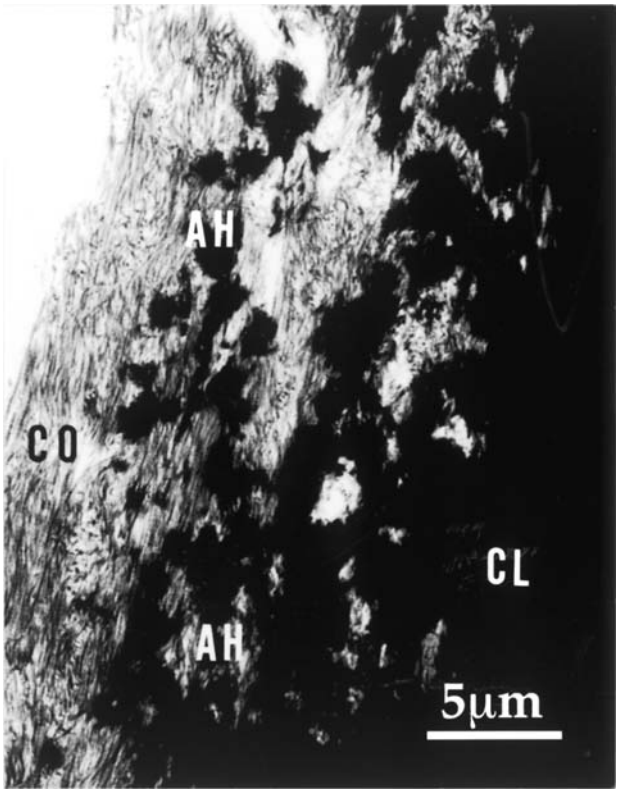

Fig. 13 Large magnification of ✱ area in Figure 12, globular deposition of hydroxyapatite, the crystal-axes (AH) coincide with longitudinal axes of collagen fibres (CO).

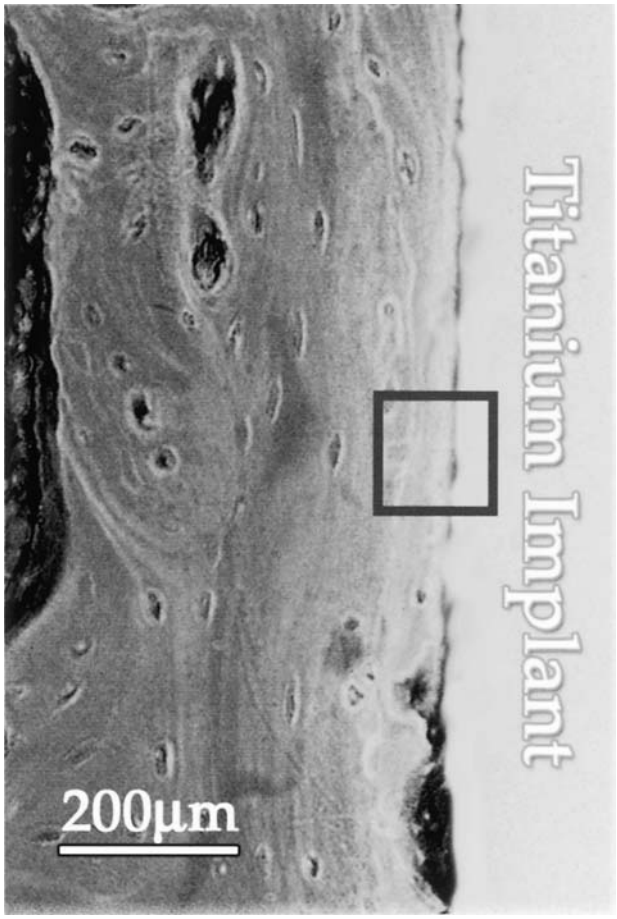

Fig. 14 Implant sheath bone surrounding titanium implant, 100 × 100 μm square for electron probe microanalysis.

is developed by cooperation of OMC originated from HSC and OSC from cortical endosteum mainly. Many studies have confirmed that new bone layers arose from the both sides of drill-cut bone surfaces and the implant surface. Both the new bone layers adjoined closely together to make implant sheath bone [1, 2, 31–33].

The new bone layer at the implant surface could be divided into two sublayers of solution mediated caltification layer (SMCL), pseudo bone and cell mediated calcification layer (CMCL), true bone [34, 35]. SMCL was formed by deposition of calcium and phosphorus into the cellular remnants of HSC; erythrocytes, platelets, monocytes macrophages, osteomediator cells, etc. (Fig. 6, 10, 11). At the early stage, up to 3 weeks post implantation, these HSC contacted closely to the implant surface with 20–100 nm thick electron dense membrane [21–24], consisting Ti, Ca, P and macromolecular substances [30, 35].

6 weeks post implantation: As time proceeds SMCL developed the calcium deposition by solution-mediated calcification and changed to the pseudo bone. The outside of SMCL combined seamlessly to the new bone of CMCL (Figs. 12–13). Electron probe analysis of calcium and phosphorus in SMCL demonstrated the presence of phosphorus-deficient calcified layer of 5–40 μm thickness, Ca/P ratio 4.17, compared with Ca/P ratio 1.5–1.7 of true bone, CMCL (Figs. 14–16). Therefore OMC was hardly seen in the SMCL at 6 weeks post implantation, because of completion of solution-mediated calcification in the OMC-remnants. Osteoblasts were arranged in parallel to the implant surface with intervenient layers of extracellular matrix, collagen fibres layer, CMCL and SMCL (Fig. 12). Direct apposition of mineralized tissue of SMCL and CMCL appears to be an inevitable phenomenon, similar to connective tissue encapsulation of foreign-body reaction in soft tissue. Finally, the new bone layer closely jointed to young bone layer originated from the adjacent bones (cortical or trabecular) and formed the implant-sheath-bone.

This morphological study explained that bone healing process at the implant/bone marrow interface is delayed more with longer distance from the endosteum of cortical bone. The bone formation around the implants depends upon mainly the OSC migration from the cortical endosteum to the implant surface. Unfortunately this study could not clarified the topographic dependency on the bone formation at the implant/bone marrow interface between SR,Ra0.4 $\pm$ 0.01 μm and LR, Ra2.0 $\pm$ 0.12 μm.

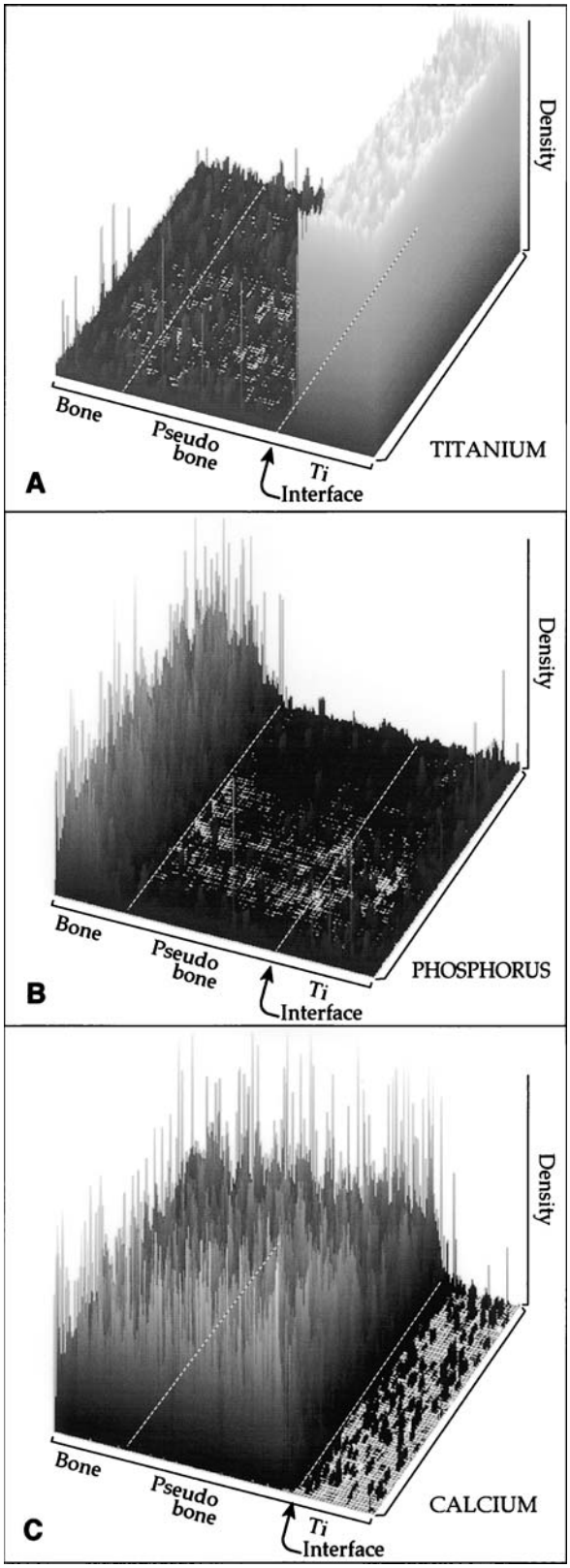

Fig. 15 Electron probe microanalysis of the titanium implant and bone marrow interface, 100 × 100 μm square in Figure 14, **A** : Titanium, **B** : Phosphorus, **C** : Calcium, Ti : titanium implant, Pseudo bone : solution-mediated calcification layer, Bone : osteoblast-mediated calcification layer.

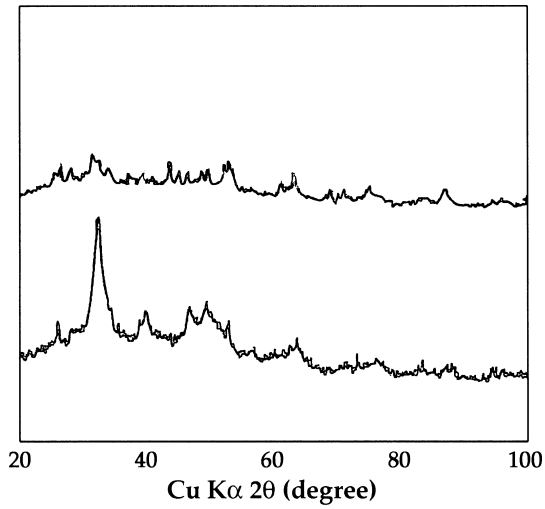

Fig. 16 X-ray diffraction patterns at the true bone layer (lower) and pseudo bone (upper).

Conclusion

TEM of the implant/bone marrow interface demonstrates that OMC release growth factors of cytokine like substances for OSC differentiation to osteoblast at the implant/bone marrow interface. Osteoblasts develop HA-deposition in collagen fibre layer around the implants. At 42 days post implantation, OMC degenerate to the cell-remnants and change to pseudo bone by solution-mediated calcification.

It is revealed that growth rate of the implant-sheath-bone depends upon the two factors of marrow space (distance from the implant surface to cortical endosteum) and healing potentiality of HSC and OSC migrated to the implant surface. These two factors have a wide variation and conceal the significant difference among the bone formations on different surface topographies. In vivo data hardly demonstrate the significant differences unlike in vitro examination, especially under the biting load of functional mastication. It is natural that the experimental data obtained in macro-environment in vivo of open system is quite different from that in micro-environment, in vitro of close system.

References

1. H. KAWAHARA, D. KAWAHARA, M. HAYAKAWA, Y. TAMAI, T. KUREMOTO and S. MATSUDA, *Impl. Dent.* **12** (2003) 61.
2. H. KAWAHARA, M. TAKAHASHI, H. AOKI, H. KOIKE, D: KAWAHARA and S. MATSUDA, *JMSM*, in press, 2006.
3. H. KAWAHARA, Y. SOEDA, K. NIWA, M. TAKAHASHI, D. KAWAHARA and N. ARAKI, *JMSM.* **15** (2004) 1261.

4. Y. MIMURA and H. KAWAHARA, In Proceedings of the 26*th* International Meeting of Implantology and Transplantology, Bologna, 1996, edited by G. Muratori 7.
5. W. ROBERTS, R. SMITH, Y. ZILBERMAN, P. MOZSARY and R. SMITH, *Am. J. Orthod.* **86** (1984) 95.
6. V. GROSS, H.-J. SCHMITZ and V. STRUNZ, in "Bioceramics: Materials Characterization vs in Vivo Behavior" N.Y. Academy of Science, N.Y., (1988) 211.
7. L. SENNERBY, P. THOMSON and L. ERICSON, *J. Mater Sci: Mater. Med.* **4** (1993) 240.
8. L. SENNERBY, P. THOMSON and L. ERICSON, *J. Mater Sci: Mater. Med.* **4** (1993) 494.
9. H. KAWAHARA, in "Encyclopedic Handbook of Biomaterials and Bioengineering" Part B, edited by D. L. WISE, D. J. TRANTOLO, D. E. ALTOBELLI, M. J. YASZEMSKI, J. D. GRESSER and E. R. SCHWARTZ Marcel Dekker Inc., New York, (1995) 1469.
10. R. SINGHVI, G. STEPHANOPOULOS and DIC. WANG, *Biotechnol. Bioeng.* **43** (1994) 764.
11. H. LIAO, A.-S. ANDERSSON, D. SUTHERLAND, S. PETRONTS, B. KASEMO and P. THOMSEN, *Biomater.* **24** (2003) 649.
12. J. Y. MARTIN, Z. SCHWARTS, T. W. HUMMER, D. M. SCHRAUB, J. SIMPSON, J. JR. LANKFORD, D. D. DEAN, D. L. COCHRAN and B. D. BOYAN, *JBMR.* **29** (1995) 389.
13. K. ANSELME, M. BIGERELLE, B. NOËL, E. DUFRESNE, D. JUDAS, A. IOST and P. HARDOUIN, *JBMR.* **49** (2000) 155.
14. K. ANSELME, M. BIGERELLE, B. NOËL, A. IOST and P. HARDOUIN, *JBMR.* **60** (2002) 529.
15. D. PERIZZOLO, W. R. LACEFIELD and D. M. BRUNETTE, *JBMR.* **56** (2001) 498.
16. B. D. BOYAN, C. H. LOHMANN, M. SISK, Y. LIU, V. L. SYLVIA, D. L. COCHRAN and D. D. DEAN, *JBMR.* **22** (2001) 350.
17. A. KIRSCH and K. DONATH, Fortschritte der Zahn Ärztlichen Implantologie. **1** (1984) 35.
18. K. A. THOMAS and S. COOK, *JBMR.* **19** (1985) 875.
19. S. G. STEINEMANN, J. EULENBERGER, P. A. MÄAUSLI and A. SCHROEDER, in "Advances in biomaterials" (Elsevier, Amsterdam, 1986) 409.
20. M. S. BLOCK, J. N. KENT and J. F. KAY, *J. Oral Maxillofac. Sur.* **45** (1987) 601.
21. M. WEINLAENDER, E. B. KENNEY, V. LEKOVIC and P. K. MOY, *Int. J. Oral Maxillofac. Impl.* **7** (1992) 491.
22. A. WENNERBERG, T. ALBREKTSSON, B. ANDERSSON and J. J. KROL, *Clin. Orallmpl. Res.* **6** (1995) 24.
23. R. K. PERRY, R. D. NISHIMURA, M. ADACHI and A. CAPUTO, *Clin. Oral Impl. Res.* **8** (1997) 442.
24. D. BUSER, T. NYDEGGER, T. OXLAND, D. L. COCHRAN, R. K. SCHENK, H. P. HIRT, D. SN ETIVY and L.-P. NOLTE, *JBMR.* **45** (1999) 75.
25. C. LARSSON, M. ESPOSITO, H. LIAO and P. THOMSEN, in Titanium in Medicine: Pringer, Berlin, (2001) 587.
26. W. J. A. DEHERT, P. THOMSEN, A. BLOMGREN, M. ESPOSITO, L. ERICSON and A. VERBOUT, *JBMR.* **41** (1998) 574.
27. H. KAWAHARA, Y. TAKASHIMA, AA. TOMINAGA and K. TAN, in Oral Implantology and Biomaterials, edited by H. KAWAHARA Elsevier, Amsterdam, (1989) 177.
28. Y. AYUKAWA, F. TAKESHITA and M. YOSHINARI, *J. Periodont.* **69** (1998) 62.
29. H. M. FROST, *Anat. Reco.* **219** (1987) 1.
30. J. W. BUDD, K. NAGAHARA, K. L. BIELAT, M. A. MEENAGHAN and N. G. SHAAF, *Int. J. Oral Maxillofac. Impl.* **7** (1992) 151.
31. H. KAWAHARA, T. MATSUDA and D. KAWAHARA, *J. Oromax. Biomech.* **6** (2000) 66.
32. H. KAWAHARA, *JJSB.* **18** (2000) 3.
33. B. CONSTANTZ, I. ISON and M. FULMER, *Sci.* **267** (1995) 1796.
34. M. TUNG and W. BROWN, *Calcif. Tissue Int.* **37** (1985) 329.
35. D. KAWAHARA and H. OHNO, in Materials in Clinicaal Application III, edited by P. VINCENZINI and R. BARBUCCI (CIMTEC 2002, Florence) 447.